Temperature dependence of the critical current of the superconducting microladder in zero magnetic field: Theory and experiment

H. J. Fink
Department of Electrical Engineering and Computer Science, University of California, Davis, Davis, California 95616

O. Buisson* and B. Pannetier
Centre de Recherches sur les Très Basses Température, Centre National de la Recherche Scientifique, Boîte Postale 166X, 38042 Grenoble CEDEX, France

(Received 25 June 1990; revised manuscript received 10 December 1990)

The largest supercurrent which can be injected into a superconducting microladder was calculated as a function of nodal spacing $\mathcal{L}$ and temperature for zero magnetic flux using (i) exact solutions of the Ginzburg-Landau equation in terms of Jacobian elliptic functions and (ii) approximate solutions in terms of hyperbolic functions. The agreement is good for $\mathcal{L}/\xi(T)<3$, where $\xi(T)$ is the temperature-dependent coherence length. Since solution (ii) is much simpler than solution (i), it is of considerable value when calculating critical currents of micronets with nodal spacings comparable to $\xi(T)$. We find that the temperature-dependent critical current deviates significantly from the classical $\frac{3}{2}$ power law of the Ginzburg-Landau theory. Preliminary experiments on a submicrometer ladder confirm such deviations.

I. INTRODUCTION

When one deals with currents, internal as well as external, in superconducting microcircuits, the full nonlinear Ginzburg-Landau (GL) equations have to be employed. The impact of the nonlinear term in the GL theory on the critical current of a long thin wire is discussed in Ref. 1. Critical-current calculations have been published for an infinite superconducting square network in zero magnetic field,[2] for a superconducting wire with very long side branches,[3] for a superconducting quantum interference device (SQUID),[4] and for the microladder in small magnetic fields.[5] An alternative approach, using eigenvalues of the linearized GL equations, which are related to $\mathcal{L}/\xi(T)$, was explored by the authors of Refs. 6–8. The temperature-dependent GL coherence length is $\xi(T)$.

Our work, concerning the square ladder in zero field, can be reduced to an investigation of the critical current of a thin wire with side branches of length $\mathcal{L}/2$, where $\mathcal{L}$ is the distance between the nodes. As shown in Figs. 1(a) and 1(b), half of the ladder corresponds to a wire with side branches. In the center of a transverse branch, the modulus of the order parameter $f(x)$ has a maximum, while at the center of the longitudinal branches $f(x)$ has a minimum in the presence of a current. These extrema are denoted by f_{02} and f_{01} and the corresponding $f(x)$'s are depicted schematically in Fig. 1(c), with f_n being the value of $f(x)$ at node n. The nodal conditions require that all order parameters (OP's) of all branches are the same at a node, and that the derivatives of $f_i(x)$ with respect to x, taken radially outward from a node and summed over all branches i, is zero.

It is our goal to find $f(x)$ using the nonlinear GL equations such that $f(x)$ has extrema, distance $\mathcal{L}/2$ from a node, with current flowing in two of the branches while none is flowing in the third. The maximum current which permits such a solution is the critical current. The same approach applies to the approximate solution.

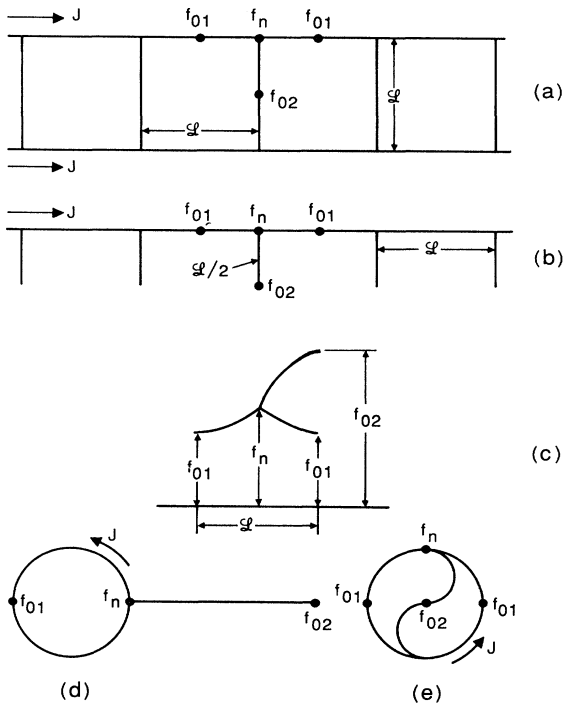

FIG. 1. Shown is the ladder: (a) f_{01} is the minimum of $f(x)$ in the current-carrying branch, f_{02} is the maximum in the branch without a current, and f_n is the value at a node; (c) schematic $f(x)$ for (a). (b), (d), and (e) are circuits with equivalent $f(x)$ distributions to those in (a).

It is of interest to note that circuits like those in Figs. 1(d) and 1(e), linked by a magnetic flux, have the same spatial configuration of $f(x)$ as shown in Fig. 1(c). However, the persistent current in the loops, linking the flux, is an internal current in the latter two circuits, while for Figs. 1(a) and 1(b) the current is from an external source. Since the currents in each branch of the ladder are the same, the flux linking a unit cell is zero when an external current is present. There are no persistent currents for zero-flux linkage.

Section II treats the exact solution of the critical current. In Sec. III we propose an approximate solution, and Sec. IV deals with the experimental results and their comparison with theory.

II. EXACT SOLUTION

We assume that the thickness of the wires of the uniform microladder is comparable to, or smaller than, $\xi(T)$ and the penetration depth $\lambda(T)$. We may, therefore, use the one-dimensional GL equations

$$\xi^2\frac{d^2f}{dx^2}+(1-f^2-q^2)f=0 , \tag{1a}$$

$$J=f^2q , \tag{1b}$$

where $q(x)$ is the normalized *gauge-invariant* superfluid velocity defined by

$$q(x)=\xi\frac{d\theta}{dx}+A_x$$

and J is the normalized current density. The phase of the complex OP is θ and A_x is the component of the normalized vector potential parallel to the coordinate x. The vector potential associated with the external source is implicitly included in $q(x)$. For a thin wire the current density is assumed to be uniform across the wire so that $q(x)$ in (1a) can be replaced by J/f^2 with J being a constant in a branch. As was shown in Ref. 3, Eq. (1a) can be integrated once, yielding a first-order differential equation whose solutions are known functions. J is related to the current density in conventional cgs Gaussian units by

$$J_{\rm conv}=Jc\phi_0/(8\pi^2\xi\lambda^2) .$$

Provided that the temperature dependence of J can be ignored, $J_{\rm conv}$ is proportional to $(T_c-T)^{3/2}$ owing to $\xi(T)$ and $\lambda(T)$. The fluxoid quantum ϕ_0 is a positive constant. The present method of computation, using the exact nonlinear GL equations, is outlined in Ref. 3. It follows from Ref. 3 that $f(x)$ in the current-carrying branch *near the maximum* of J is given in terms of Jacobian elliptic functions by

$$f_1^2(x')=f_{01}^2+|R_1|{\rm sc}^2(u_1|m'){\rm dn}^2(u_1|m')$$

with

$$u_1=x'(|R_1|/2)^{1/2}/\xi ,$$

$$|R_1|^2=2[J^2/f_{01}^2-f_{01}^2(1-f_{01}^2)] ,$$

$$m'=[1+{\rm Re}(R_1)/|R_1|]/2 ,$$

$${\rm Re}(R_1)=1-3f_{01}^2/2 ,$$

and

$${\rm sc}^2(u_1|m'){\rm dn}^2(u_1|m')=[1-{\rm cn}(2u_1|m')]/[1+{\rm cn}(2u_1|m')] .$$

The coordinate $x'=0$ is located at the minimum of $f_1(x')$, where $f_1(x')=f_{01}$, and the node is located at $x'=\mathcal{L}/2$.

The transverse branch which does not carry a current has a modulus of the OP

$$f_2(x'')=f_{02}{\rm cd}(u_2|m'')$$

with

$$u_2=x''(1-f_{02}^2/2)^{1/2}/\xi ,$$

$$m_1''\equiv 1-m''=(1-f_{02}^2)/(1-f_{02}^2/2) .$$

The coordinate $x''=0$ is located at the maximum of $f_2(x'')$, where $f_2(x'')=f_{02}$, and the node is located at $x''=\mathcal{L}/2$. The nodal conditions are

$$f_1^2(\mathcal{L}/2)=f_2^2(\mathcal{L}/2)$$

and

$$2|df_1^2/dx'|=|df_2^2/dx''|$$

at $x'=x''=\mathcal{L}/2$. With the notation (u) for $(u|m)$, these are, explicitly,

$$f_{01}^2+|R_1|[1-{\rm cn}(2u_1)]/[1+{\rm cn}(2u_1)]=f_{02}^2{\rm cn}^2(u_2)/{\rm dn}^2(u_2) , \tag{2}$$

$$(32)^{1/2}|R_1|^{3/2}\frac{{\rm sn}(2u_1){\rm dn}(2u_1)}{[1+{\rm cn}(2u_1)]^2}=2m_1''f_{02}^2(1-\tfrac{1}{2}f_{02}^2)^{1/2}\frac{{\rm sn}(u_2){\rm cn}(u_2)}{{\rm dn}^3(u_2)} . \tag{3}$$

The current density J is embedded in $|R_1|$. Equations (2) and (3) were solved numerically, finding f_{01} and f_{02} for fixed values of $\mathcal{L}$ and J.

Figures 2 and 3 show the general elliptic-function solutions for two different lattice spacings, where we have plotted J as a function of the moduli of the OP's at the node and at the extremal values. As the current is increased from zero, $f(x)$ decreases from unity. The decrease is more rapid in the longitudinal (f_{01}) than in the transverse branch (f_{02}). When the maximum value of J, J_c, is exceeded by the external source, the ladder is driven into the normal or phase-slip state. Therefore, J_c is the normalized critical-current density (per wire) of the ladder. The curves to the left of the maxima are unphysical when only applied currents are present, but have physical significance if J is a persistent current due to

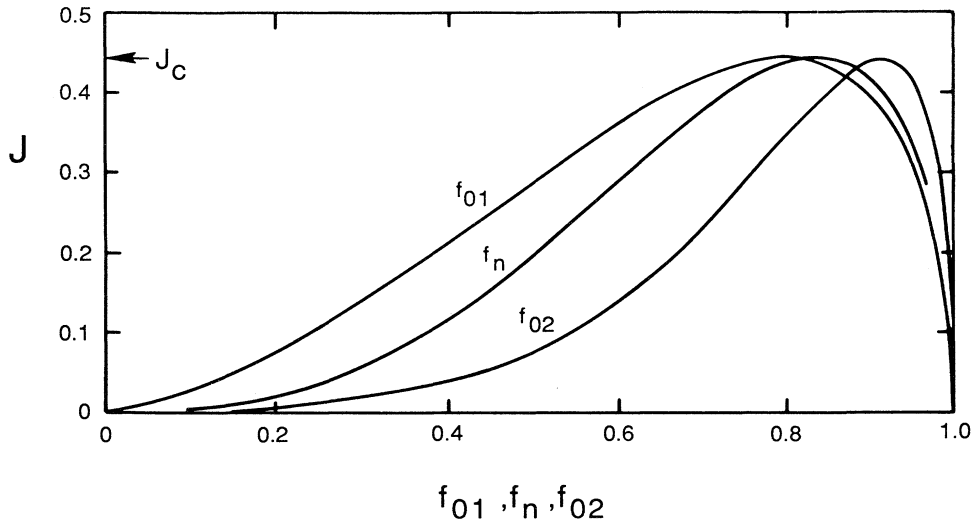

FIG. 2. Normalized current density J, injected into the circuit of Fig. 1(b), as a function of the $f(x)$'s at the extrema and the node for $\mathcal{L}/\xi=0.6\pi$. Here $J_c=0.4435$.

magnetic flux linking the circuit. Figure 2 is characteristic for lattice spacing $\mathcal{L}/\xi \lesssim 0.6\pi$ and Fig. 3 is characteristic for $\mathcal{L}/\xi \gtrsim 0.8\pi$.

Figure 4 summarizes the values of J_c obtained from plots similar to the two previous figures. The encircled points are values calculated from Eqs. (2) and (3). It should be noted that J_c is normalized, that the current in conventional units includes a $(T_c-T)^{3/2}$ term, and that the horizontal axis is a function of temperature. Thus, if $\mathcal{L}/\xi(T)$ changes, for example, from 0 to 4 as the temperature is changed, the temperature dependence of J_c must necessarily differ from the classical $(T_c-T)^{3/2}$ dependence. As $\mathcal{L}/\xi \to 0$, the value of $J_c \to \sqrt{2}/3$; and as $\mathcal{L}/\xi \to \infty$, the value of $J_c \to 2/\sqrt{27}$, the normalized critical current density of a long wire without side branches.

For $\mathcal{L}/\xi \lesssim 1$ and $\mathcal{L}/\xi \gg 1$, the following limiting solutions are obtained from Eqs. (2) and (3).

A. Limit $\mathcal{L}/\xi \lesssim 1$

For $\mathcal{L}/\xi \ll 1$, we expect that $f_{01} \to f_n \to f_{02}$. In that case, both u_1 and u_2 will be small. Expanding Eq. (2) to order u_1^2 and u_2^2, one obtains

$$f_{01}^2 + |R_1| u_1^2 \approx f_{02}^2 (1 - m_1'' u_2^2)$$

or

$$f_{01}^2 + |R_1|^2 (\mathcal{L}^2/8\xi^2) \approx f_{02}^2 [1 - (1 - f_{02}^2)(\mathcal{L}^2/4\xi^2)] \ . \quad \text{(2a)}$$

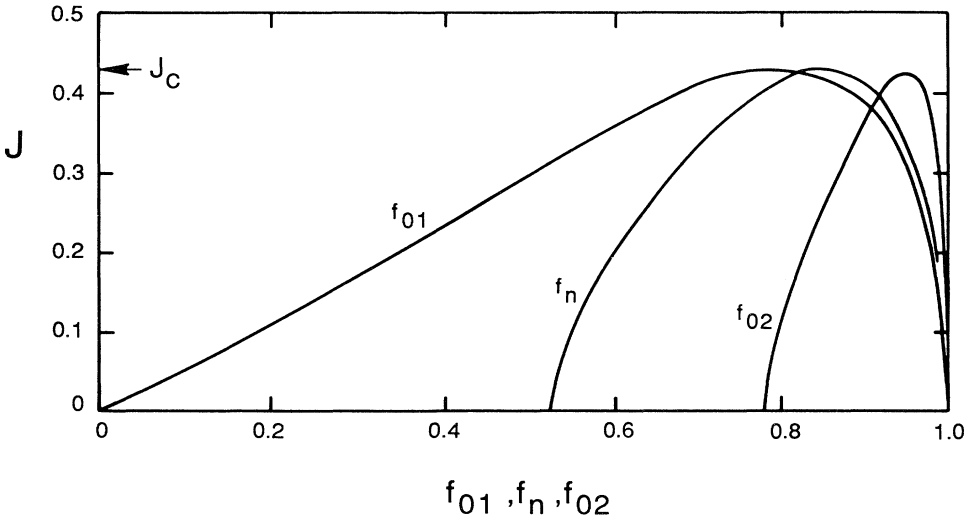

FIG. 3. Similar to Fig. 2 except $\mathcal{L}/\xi=0.8\pi$ and $J_c=0.4305$.

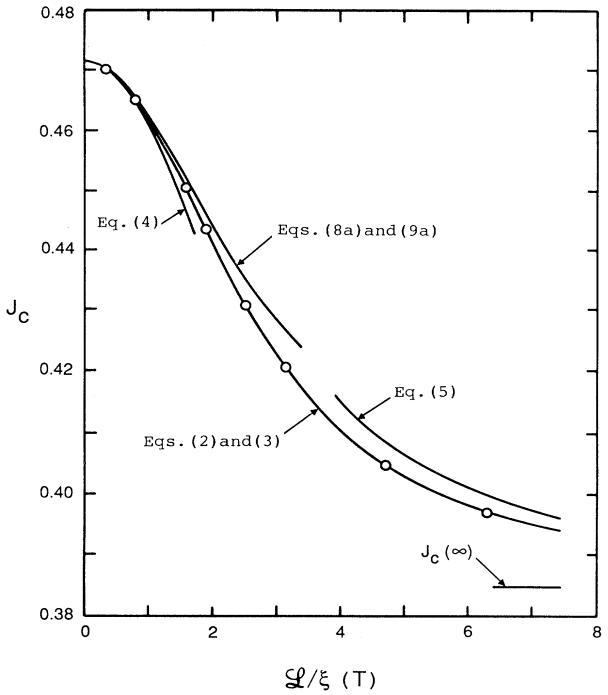

FIG. 4. Temperature-dependent size correction of the critical-current density of a microladder in zero magnetic field. Equations (2) and (3) refer to the exact results, Eqs. (4) and (5) refer to the limiting results for $\mathcal{L}/\xi \lesssim 1$ and $\mathcal{L}/\xi \gg 1$, respectively, and Eqs. (8a) and (9a) refer to the hyperbolic approximation.

Similarly, for Eq. (3),

$$|R_1|^2(\mathcal{L}/\xi) \approx f_{02}^2(1-f_{02}^2)(\mathcal{L}/\xi) \ . \tag{3a}$$

For $\mathcal{L}/\xi \neq 0$, we replace $f_{02}^2(1-f_{02}^2)$ in Eq. (2a) by $|R_1|^2$ from Eq. (3a) and solve for

$$f_{02}^2 = f_{01}^2 + 3|R_1|^2(\mathcal{L}^2/8\xi^2) \ .$$

The value of f_{02}^2 in Eq. (3a) is now replaced by the latter equation which becomes a function of $|R_1|$ and f_{01} only. Replacing $|R_1|$ by its definition, the remaining equation contains only J, f_{01}, and $\mathcal{L}/\xi$. Maximizing J with respect to f_{01} for fixed $\mathcal{L}/\xi$, the critical current for $\mathcal{L}/\xi \lesssim 1$ is

$$J_c = \tfrac{1}{3}\sqrt{2}\left[1-\frac{1}{48}\left[\frac{\mathcal{L}}{\xi}\right]^2\right] . \tag{4}$$

This equation is shown also in Fig. 4.

B. Limit $\mathcal{L}/\xi \gg 1$

One expects that $f_{02} \to 1$ as $\mathcal{L}/\xi \to \infty$. Assume that $\mathcal{L}/\xi \gg 1$, then $|m_1''| \ll 1$. Then, the functions on the right-hand side of Eqs. (2) and (3) can be expanded in terms of hyperbolic functions, with only the exponential functions with positive exponents remaining for large values of $\mathcal{L}/\xi$. The result is

$$\mathrm{cn}(u_2)/\mathrm{dn}(u_2) = (1-z)/(1+z) \ ,$$

$$m_1''\,\mathrm{sn}(u_2)\mathrm{cn}(u_2)/\mathrm{dn}^3(u_2) = (4+m_1'')z(1-z)/(1+z)^3 \ ,$$

where we have used the definition $z = m_1''\exp(2u_2)/16$. Furthermore,

$$2u_2 = \mathcal{L}(1-f_{02}^2/2)^{1/2}/\xi \approx \mathcal{L}/\sqrt{2}\xi \ .$$

The latter functions of z are well behaved for any value of z, but we expect z to be small compared to unity for $\mathcal{L}/\xi \gg 1$. Similarly, we expect

$$2u_1 = \mathcal{L}(|R_1|/2)^{1/2}/\xi$$

to be small compared to unity in Eqs. (2) and (3), meaning that $|R_1|^{1/2}$ decreases as rapidly as $\mathcal{L}/\xi$ increases. Then, Eqs. (2) and (3) to order u_1^2 are

$$f_{01}^2 + |R_1|^2(\mathcal{L}^2/8\xi^2) \approx f_{02}^2(1-z)^2/(1+z)^2 \ , \tag{2b}$$

$$|R_1|^2(\mathcal{L}/\xi) \approx 2f_{02}^2(1-\tfrac{1}{2}f_{02}^2)^{1/2}(4+m_1'')z(1-z)/(1+z)^3 \ . \tag{3b}$$

For $z \ll 1$, the right-hand side of Eq. (2b) is $f_{02}^2(1-4z)$ and Eq. (3b) (with $f_{02} \to 1$) becomes

$$|R_1|^2\mathcal{L}/\xi \approx 4\sqrt{2}z \ .$$

Replacing the right-hand side of Eq. (2b), namely,

$$f_{02}^2(1-4z) \ \text{ by } \ 1-|R_1|^2(\mathcal{L}/\sqrt{2}\xi) \ ,$$

one obtains an expression which depends on J, f_{01}, and $\mathcal{L}/\xi$ only. Maximizing J with respect to f_{01} for fixed $\mathcal{L}/\xi$, one obtains

$$J_c \approx \frac{2}{\sqrt{27}}\left[1+\frac{3}{(\mathcal{L}/\xi)(\mathcal{L}/\xi+4\sqrt{2})}\right] . \tag{5}$$

Equation (5) is also shown in Fig. 4. Equations (4) and (5) are reasonable fits to the exact results in the small- and large-$(\mathcal{L}/\xi)$ limits.

III. APPROXIMATE SOLUTION

Here we introduce a scheme for obtaining approximate critical-current densities and compare the results with the exact results of Fig. 4. In Ref. 3 it was shown that, after replacing the superfluid velocity in the first GL equation by the current density, the latter equation could be integrated once. With the definitions $f_1^2(x) = f_{01}^2 + t^2(x)$ for the current-carrying branch and $f_2^2(x') = f_{02}^2 - v^2(x')$ for the branch without a current, Eq. (3) of Ref. 3 becomes

$$\xi^2\left[\frac{dt}{dx}\right]^2 = b^2 + a_1^2t^2 + \tfrac{1}{2}t^4 \tag{6a}$$

and

$$\xi^2\left[\frac{dv}{dx'}\right]^2 = c^2 + a_2^2v^2 + \tfrac{1}{2}v^4 \ , \tag{6b}$$

where

$$a_1^2=\tfrac{3}{2}f_{01}^2-1\ ,$$

$$a_2^2=\tfrac{3}{2}f_{02}^2-1\ ,$$

$$b_2=J^2/f_{01}^2-f_{01}^2(1-f_{01}^2)\ ,$$

$$c^2=f_{02}^2(1-f_{02}^2)\ .$$

If we assume that $t^2\ll 2|a_1^2|$ and $v^2\ll 2|a_2^2|$, we may neglect the t^4 and v^4 terms in Eqs. (6a) and (6b), respectively. The solutions of Eqs. (6a) and (6b) then become

$$t=\frac{b}{a_1}\sinh(a_1x/\xi) \tag{7a}$$

and

$$v=\frac{c}{a_2}\sinh(a_2x'/\xi)\ . \tag{7b}$$

The coordinate $x=0$ is located at the minimum and $x'=0$ is at the maximum of $f(x)$. The node is a distance $\mathcal{L}/2$ from the extrema. The nodal conditions

$$f_{01}^2+t^2(\mathcal{L}/2)=f_{02}^2-v^2(\mathcal{L}/2) \tag{8}$$

and

$$2\left[\frac{dt^2}{dx}\right]_{x=\mathcal{L}/2}=\left[\frac{dv^2}{dx'}\right]_{x'=\mathcal{L}/2} \tag{9}$$

lead to the following set of equations:

$$f_{02}^2-f_{01}^2=\left[\frac{b}{a_1}\right]^2\sinh^2(a_1\mathcal{L}/2\xi)+\left[\frac{c}{a_2}\right]^2\sinh^2(a_2\mathcal{L}/2\xi)\ , \tag{8a}$$

$$2\frac{b^2}{a_1}\sinh(a_1\mathcal{L}/\xi)=\frac{c^2}{a_2}\sinh(a_2\mathcal{L}/\xi)\ . \tag{9a}$$

For fixed J and $\mathcal{L}/\xi$, Eqs. (8a) and (9a) constitute a set of equations with implicit unknowns f_{01} and f_{02}. Solutions of this set of equations for J with fixed $\mathcal{L}/\xi$ lead to curves similar to those shown in Figs. 2 and 3.

The following algorithm was used in solving the latter set of equations. Equation (9a) was solved for b and substituted into Eq. (8a). The latter is then a function of f_{01} and f_{02} only. For fixed f_{02}, the corresponding value of f_{01} was found. Then, with f_{01} and f_{02}, the value of b was obtained from Eq. (9a) and from it the current density J. This was done for a large number of f_{02} values until J reached its maximum value J_c, the critical current. A plot of the results of Eqs. (8a) and (9a) is also shown in Fig. 4. It compares favorably with the exact results for $\mathcal{L}/\xi<3$. Expanding Eqs. (8a) and (9a) for small values of $\mathcal{L}/\xi$, one obtains the same result as Eq. (4). The hyperbolic approximation is inaccurate for large values of $\mathcal{L}/\xi$.

IV. CRITICAL CURRENT AS A FUNCTION OF TEMPERATURE

Critical-current measurements on various micronetworks were performed by Buisson *et al.*[9] Results on extended networks have been reported elsewhere,[8] with emphasis on magnetic field effects. Here we consider the zero-field critical current of the microladder.

Samples were prepared by electron-beam lithography and pure aluminum liftoff.[8] Nominal characteristic sample parameters are the following: lattice spacing $\mathcal{L}=3.2$ μm, thickness $=87$ nm, and wire width $=0.35$ μm. There were 37 unit cells between voltage and 77 between current probes. Analysis of the resistivity and critical field data led to the following physical parameters: $T_c=1.253$ K (mid-height), $\xi(0)=0.21$ μm, and $R(4.2\ \text{K})=17.8\ \Omega$. More details of the experimental techniques are given in Refs. 8 and 9. The critical current is determined for each temperature from the I-V characteristics with a threshold voltage criterion of 200 nV.

For the purpose of comparing our experimental results with our theoretical calculations, we note that the exact results of Fig. 4 can be approximated by

$$J_c=C(T)J(\infty)\ ,$$

with

$$C(T)=1+\frac{0.224\,74}{\cosh^2[5.5(1-t)^{1/2}]}\ , \tag{10}$$

where $J(\infty)$ is the current density of a single long wire without any side branches. Equation (10) represents a very good fit to the exact results of Fig. 4 for $\mathcal{L}/\xi\lesssim 3.5$. The latter equation implies that the critical current of the ladder can be viewed as the critical current of a single, long wire of effective cross-sectional area $2AC(T)$, where A is the true cross section of a single wire.

Near zero temperature, $\mathcal{L}/\xi\gg 1$ in our case, and $C(T)\to 1$ (see Fig. 4). The two longitudinal wires of the ladder become decoupled from each other and, therefore, the critical current is just twice the critical current of a long single wire of value

$$I_0=[(c\phi_0)/(4\pi^2\sqrt{27})]\{A/[\xi(0)\lambda^2(0)]\}\ .$$

In the other limit, when $T\to T_c$ and $\mathcal{L}/\xi\ll 1$, the transverse branches enhance coupling between the longitudinal wires, thereby increasing the effective cross section $2AC(T)$ to $A\sqrt{6}$.

The experimental critical current of the ladder shows a deviation from the $\frac{3}{2}$ power law. This is illustrated in Fig. 5 where we have plotted the ratio $I_c/[2I_0(1-T/T_c)^{3/2}]$ versus reduced temperature. The current I_0 is the zero-temperature critical current of a single long wire. This ratio allows a direct comparison with the theoretical function $C(T)$, Eq. (10). Since this ratio is very sensitive to the choice of T_c, we use both T_c and I_0 as adjustable parameters. This adjustment of T_c is necessary since the $R(T)$ curve provides the critical temperature only to an accuracy limited by the width of the resistive transition, which was about 2 mK. This accuracy is insufficient for a comparison of theory and experi-

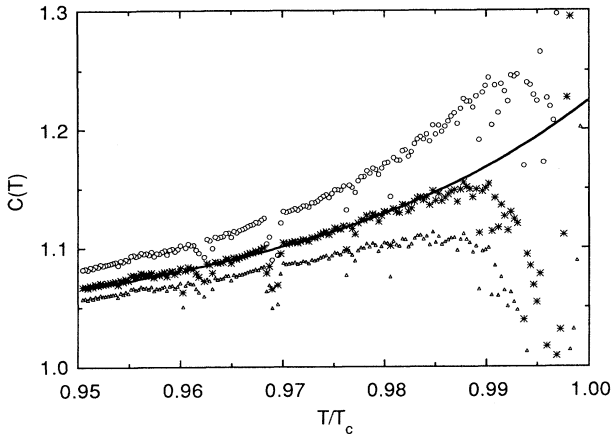

FIG. 5. Dependence of the function $C(T)$, Eq. (10), on the reduced temperature T/T_c (continuous line). Experimental data are plotted as $I_c/[2I_0(1-T/T_c)^{3/2}]$, the measured critical current I_c of the ladder, divided by twice the GL critical current of a single long wire. Best-fit parameters are $I_0=4.75$ mA and $T_c=1.2492$ K. Note the sensitivity of the data to the choice of T_c: 1.2486 (open circles), 1.2492 (stars), and 1.2496 K (triangles).

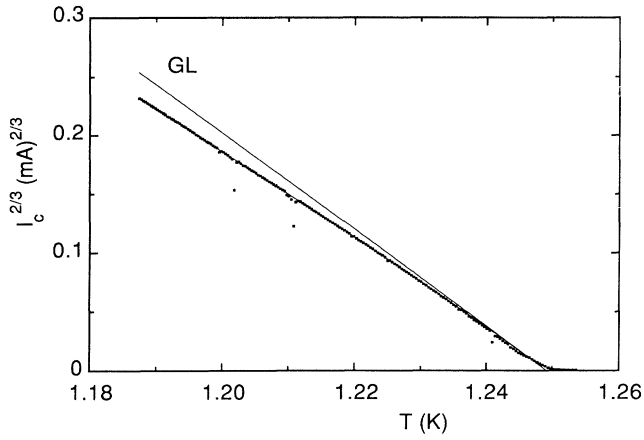

FIG. 6. Plot of $I_c^{2/3}$ vs T. Crosses show experimental data (same data as in Fig. 5). The continuous line through the points is the theoretical curve $I_c^{2/3}=[2I_0C(T)]^{2/3}(1-T/T_c)$ for best-fit values $I_0=4.75$ mA and $T_c=1.2492$ K. Also shown is the asymptotic limit, plotted with $C(T)=1.224$, denoted by GL, which is valid for $\mathcal{L}/\xi \ll 1$.

ment. The crosses correspond to best-fit parameters $I_0=4.75$ mA and $T_c=1.2492$ K. We obtain a good fit of our experimental data to the theoretical function, Eq. (10), except very near T_c. The value of the zero-temperature critical current obtained this way corresponds to a current density of 1.59×10^{11} A/m^2, which is close to the theoretical value of 1.3×10^{11} A/m^2, calculated with the microscopic parameters $\xi(0)=0.21$ μm and $\lambda(0)=70$ nm. The discrepancy between theory and experiment in the region very close to T_c is most likely due to fluctuation effects which are not taken into account in the mean-field GL theory. The agreement between theory and experiment is quite good for $T<1.234$ K, which corresponds to $\mathcal{L}/\xi(T)>1.7$.

The reader should notice the sensitivity of the fitting process to the choice of the parameter T_c. In Fig. 5, open circles and triangles correspond to T_c of 1.2486 and 1.2496 K, respectively. A conclusive test of the above theory would require an independent determination of T_c, for example, by fitting the shape of the experimental transition curve to a theoretical $R(T)$ curve, broadened by thermal fluctuations. To date, such a theory has not been published for superconducting networks.

Figure 6 shows a plot of $I_c^{2/3}$ versus T obtained with the same experimental data as shown in Fig. 5, together with the asymptotic GL theoretical curve

$$I_c^{2/3}=(I_0\sqrt{6})^{2/3}(1-T/T_c)\ ,$$

valid for $\mathcal{L}/\xi \ll 1$. The continuous line through the crosses is the theoretical curve

$$I_c^{2/3}=[2C(T)I_0]^{2/3}(1-T/T_c)$$

with $I_0=4.75$ mA and $T_c=1.2492$ K. The experimental curve accounts well for the deviation of I_c from the $\frac{3}{2}$ power law due to the size effect.

Before concluding, we note that our theory is based on an infinite ladder while the experimental ladder is finite. We expect that modifications due to the finite length of our ladder become significant only when $\xi(T)$ becomes comparable to the total length of the ladder, i.e., within a few μK near T_c.

V. CONCLUSIONS

The maximum loss-free transport current which can be injected into a superconducting microladder in zero applied magnetic field was obtained as a function of nodal spacing and temperature. Jacobian elliptic functions were used in the exact calculation of the critical current. The size and temperature corrections of the critical current are significant.

An approximate solution of the nonlinear GL equation in terms of hyperbolic functions was discovered which fits the exact solution reasonably well for $\mathcal{L}/\xi<3$. Since the latter solution simplifies the calculations considerably, it is of considerable value for critical-current calculations of micronetworks in a magnetic field, at least in the limit when the nodal distances are comparable to $\xi(T)$.

We presented preliminary experimental results on a microfabricated submicrometer aluminum ladder. The measured critical current shows a significant deviation from the classical $(T_c-T)^{3/2}$ Ginzburg-Landau dependence. Although the present theory cannot account for the details of the experimental curve over the full temperature range, we found that the low-temperature part of the $I_c(T)$ curve is well explained by our theoretical results. A complete understanding of our experiments will probably require a theoretical treatment beyond the Ginzburg-Landau framework.

ACKNOWLEDGMENTS

One of us (H.J.F.) thanks A. López for discussions and B. Pannetier for his hospitality at Grenoble. We thank M. Giroud and S. B. Haley for valuable discussions. Partial support from National Science Foundation (NSF) Grant Nos. ECS-85 05627 and INT-88 03025, and from the Université Joseph Fourier is acknowledged.

---

*Present address: Laboratorio de Materia Condensada, Dpt. Fisica, PUC, 225 rua Marquès de São Vicente, 22453 Rio de Janeiro, Brasil.

[1]M. Tinkham, *Introduction to Superconductivity* (McGraw-Hill, New York, 1975), pp. 116–120.

[2]H. J. Fink and A. López, J. Phys. Lett. (Paris) **46**, L961 (1985).

[3]H. J. Fink and V. Grünfeld, Phys. Rev. B **31**, 600 (1985).

[4]H. J. Fink, V. Grünfeld, and A. López, Phys. Rev. B **35**, 35 (1987); H. J. Fink, J. Loo, and S. M. Roberts, *ibid.* **37**, 5050 (1988).

[5]H. J. Fink and S. B. Haley, following paper, Phys. Rev. B **43**, 10 151 (1991); H. J. Fink and S. B. Haley, Phys. Rev. Lett. **66**, 216 (1991).

[6]Y. Y. Wang, B. Pannetier, and R. Rammal, J. Phys. (Paris) **49**, 2045 (1988).

[7]Y. Y. Wang, R. Rammal, and B. Pannetier, J. Low Temp. Phys. **68**, 301 (1987).

[8]O. Buisson, M. Giroud, and B. Pannetier, Europhys. Lett. **12**, 727 (1990).

[9]O. Buisson, M. Giroud, B. Pannetier, and H. J. Fink (unpublished).